Model of drop infiltration into a thin amphiphilic porous medium

Florian Cajot, Claude Doussan, Simon Hartmann, Philippe Beltrame

Journal of Colloid and Interface Science 684 (2025) 35–46

Contents lists available at ScienceDirect

Journal of Colloid And Interface Science

journal homepage: www.elsevier.com/locate/jcis

Regular Article

Model of drop infiltration into a thin amphiphilic porous medium

Florian Cajot [a,*], Claude Doussan [a], Simon Hartmann [b], Philippe Beltrame [a]

[a] UMR1114 EMMAH INRAE-AU, 228, Route de L'Aérodrome, Avignon, F84000, France
[b] Institut für Theoretische Physik, Universität Münster, Münster, D-48149, Germany

GRAPHICAL ABSTRACT

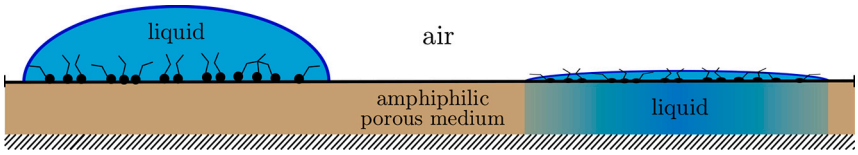

ARTICLE INFO

Keywords:
Porous media
Free energy
Interface process
Amphiphilic matter
Infiltration
Wettability
Exopolysaccharides
Rhizosphere
Soil

ABSTRACT

Hypothesis: Water drop infiltration into a thin amphiphilic porous medium is influenced by wettability. Due to the reorganization of amphiphilic matter in contact with water, polar interaction changes the wettability in the bulk porous medium and at the liquid/porous substrate interface. To model out of equilibrium water transfer, we propose a thermodynamics approach derived from Onsager's principle.
Modeling: A 2D macroscopic gradient-dynamics model coupling the drop infiltration and the water dynamic into an amphiphilic porous medium is developed and applied to rhizospheric soil in presence of exopolysaccharides (EPS) as an example. The free energy of the entire drop and porous medium system is defined by taking into account the free surface energy of the water and the effective interaction between the porous matrix and the amphiphilic matter.
Findings: The temporal evolution of the 2D drop volume and contact angle are studied during infiltration using the new formulation. Depending on amphiphilic concentrations and initial water saturation, numerical simulation captures similar scenarios to those described in the literature for powder media, as well as a latency phenomenon occurring in dry soil. The latter has been until now poorly modeled.

1. Introduction

The wettability of a porous medium is a key point for understanding water transfer in soil or in an industrial framework. This phenomenon is encountered in many applications, such as water infiltration in soil [43,66] (groundwater recharge or infiltration of rainfall water in dry soil), root irrigation of vegetation [9], ink-jet printing [21,44], textile fabrics [35], pharmacology [62] and water transport [2].

In natural environments, a number of organic molecules exhibit an amphiphilic behavior, where both hydrophilic (polar head) and hydrophobic (apolar chain) properties strongly affect wettability. Amphiphilic matter is commonly found in forest litter [60], in the soil zone around the roots, i.e. the rhizosphere which is rich in exopolysaccharides (EPS) [12,55,52] and more generally in organic matter in soils [17,34]. In dry porous media, amphiphilic matter is known to be responsible for producing a hydrophobic coating provided that the polar ends of the amphiphilic molecules are bonded to a surface such as the matrix of soil or of the porous medium [32]. In the presence of water, amphiphilic molecules spontaneously reorganize and reduce effective hydrophobicity of the medium. This amphiphilic switch has a major impact on flows, resulting in the appearance of fingering at the interface of a hydrophobic layer, water retention phenomena and intermittence [32,66]. In

* Corresponding author.
E-mail addresses: florian.cajot@gmail.com (F. Cajot), claude.doussan@inrae.fr (C. Doussan), philippe.beltrame@univ-avignon.fr (P. Beltrame).

https://doi.org/10.1016/j.jcis.2024.12.216
Received 12 July 2024; Received in revised form 23 December 2024; Accepted 27 December 2024

Available online 2 January 2025

this study, we focus on EPS as amphiphilic matter for which the water transfer model was calibrated [15]. Although the description of an amphiphilic molecule consisting of a polar head and an apolar chain does not apply to EPS, the macroscopic behavior of soil with EPS is similar to that of amphiphilic matter, notably with hydrophobic behavior at low saturation [3,50].

Modeling the behavior and impacts of amphiphilic matter and more generally of wettability has been the subject of numerous studies, particularly over the last decade. An approach consists in modeling at the pore scale the water dynamics by computing the Navier-Stokes equations for a given geometry [45,47,10,67]. Wettability is characterized by an equilibrium contact angle on the surface of the porous matrix at the pore scale. However, the challenge is to upscale wettability to the macroscale taking into account the complexity of the porous medium geometry and amphiphilic matter distribution. Other approaches are based on the Richards equation [64] governing the time evolution of water saturation in an effective continuous medium. In this approach, for simulating the specific effects of amphiphilic matter such as increase of water storage and delay of rehumectation, the hydraulic conductivity and capillary pressure functions are modified or an *ad hoc* time-dependent term is added to simulate the relaxation dynamics of the conformation change of amphiphilic molecules during imbibition. Recently, we developed a porous medium wettability model simulating various phenomena, such as water trapping, intermittent flow and fingering instability, that occur in the presence of hydrophobic matter [6]. This approach can be applied to amphiphilic media and specifically to sand with EPS to reproduce its buffer effect on water dynamics experimentally observed [15,14]. The governing flow equation is a gradient dynamics as in the Richards model but in which a wettability term replaces the suction (or matric potential) term, which accounts for the effective hydrophobic action of the amphiphilic matter. The wettability term is similar to a disjoining pressure for partial wetting as described in [36,29] which represents attractive and repulsive interactions between the porous matrix and the water free surface. The wettability depends on the water content which is a specific property of amphiphilic properties. The key point of this model is the construction of a free energy functional for the whole system studied.

The aim of this study was to develop a model of drop infiltration into an amphiphilic porous media able to reproduce both the drop dynamics on the porous medium and water transfer in this medium. Indeed, the wettability of porous media is often quantified by the infiltration duration of a drop into the porous medium. The Water Drop Penetration Time (WDPT) method is one of the most widely used [31,27,56,20]. Depending on the drop infiltration time into a substrate, the medium is ranked from hydrophilic to hydrophobic with different levels.

Models of drop infiltration into a porous medium are usually based on the Washburn law, where the porous medium is represented by a bundle of parallel cylindrical tubes in which flow takes place [39,35]. The wettability of the porous layer is taken into account by a contact angle and such models of hydrophobic porous media have been developed to determine the spontaneous infiltration of a drop into a hydrophobic porous medium [68,20]. The drop spreading may influence infiltration dynamics particularly with surfactant solution [68]. The drop dynamics is often simulated by the lubrication model [61] combined with a contact angle at the triple line. Different regimes of infiltration are identified in the literature depending on the characteristic of spreading and infiltration times [21,54,18]. An influence of the initial moisture of the porous medium is also shown [21,69].

However, in presence of amphiphilic matter, the interface is a key point in infiltration phenomena [26]. The amphiphilic matter alters the physico-chemistry of the medium [19,27], which affects the wettability within the porous medium and at the liquid/porous medium interface [32,56,26]. The water content in a porous medium influences the wettability at the interface between the drop and the substrate and impacts the timing and infiltration stages of the liquid [28,44]. This change in wettability at the interface and within the porous layer, while essential, is overlooked.

In the present study, we aim to apply the common approach developed both for the dynamics of thin liquid films [70] and for the diffusion of water in a porous medium [6,14,15]. We restrict the study to thin porous medium in order to have a one-dimensional modeling and to highlight interface phenomena. Evolution equations are written as a gradient dynamics governed by the free energy functional in each medium, the drop and the porous medium [74,6,15] containing adsorbed amphiphilic matter. The coupling between the droplet and porous media is addressed in a similar way to recent studies examining drops behavior on a polymer brush [71,40,38,48]. Exchanges and coupling terms between the two media are constrained by Onsager's variational principle [33]. The advantage of developing our model within this theoretical framework is that the out-of-equilibrium processes that occur remain consistent with thermodynamics.

The paper is organized as follows. In Section 2, first, we describe the model of the infiltration of a drop on a porous medium containing adsorbed amphiphilic matter. In Section 3, we simulate the various stationary states and imbibition dynamics of a drop deposited on a mixture of sand and EPS concentration. These results are compared with the literature results. Finally, we provide some concluding remarks in Section 4.

2. Modeling

2.1. Outline of the problem

We consider a 2D drop placed on a porous medium, of length $2L$ and thickness D, in the plan (Ox, Oz). The porous medium contains an adsorbed concentration c of amphiphilic matter. The concentration c is defined as the mass of dry amphiphilic matter per 100 g of dry substrate. This dimensionless variable is expressed without the percentage symbol. The liquid is incompressible with a density ρ and dynamic viscosity μ. The free surface of the drop is defined by a water height $\zeta(x,t)$. We note γ the liquid-air surface tension. Throughout the paper, submillimetric droplet is modeled by a continuous water thin film where a drop coexists with an ultra-thin liquid film [70,5].

As an example, in the article we will consider a porous medium which is an unsaturated homogeneous sand with a porosity $\phi = 0.43$ [52], water as the liquid and EPS as the amphiphilic matter. The concentration c is ranged in this study from 0 to 1 as experimental data [51,52] and the concentration close to the rhizosphere [75]. We define a mean saturation $s(x,t)$ over the thickness D and the equivalent height of water

$$\xi(x,t) = D\phi s(x,t) \tag{1}$$

in the thin porous medium and we neglect the water dynamics in z direction. A sketch of the considered geometry is shown in Fig. 1. All parameters of the problem are defined in Table 1.

This system can be interpreted as a thermodynamic system with two media: water on the porous medium and a heterogeneous medium constituted of porous matrix, water and amphiphilic matter. We neglect the evaporation in the two media. We associate to each medium a free energy functional depending on the order parameter ζ for the free energy in the film $\mathcal{F}^{\zeta}$ and ξ for the free energy in the soil $\mathcal{F}^{\xi}$. Because of interaction between the two media, we consider a third free energy functional $\mathcal{F}^{int}$ depending on both parameter orders ξ and ζ. This term is interpreted as the interface energy between the drop and the sand. The Helmholtz free energy $\mathcal{F}$ in the closed system is then the sum of three terms:

$$\mathcal{F} = \mathcal{F}^{\zeta} + \mathcal{F}^{\xi} + \mathcal{F}^{int}. \tag{2}$$

Each energy term $\mathcal{F}^{\square}$ has an associated $f^{\square}$ energy density and then

$$\mathcal{F} = \int_{\Omega} \left[f^{\zeta} + f^{\xi} + f^{int} \right] \mathrm{d}x, \tag{3}$$

Journal of Colloid And Interface Science 684 (2025) 35–46

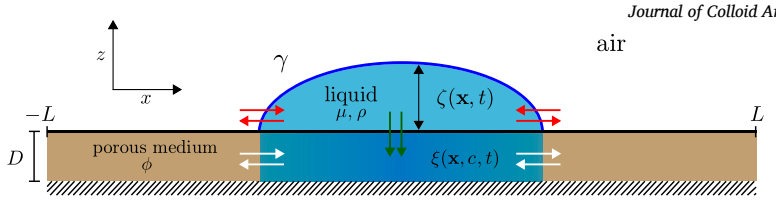

Fig. 1. Sketch of the considered geometry for a liquid drop on a soil containing amphiphilic matter. The colored arrows represent the dynamics studied: the spreading/retracting of the drop on the amphiphilic soil (red), the water drop infiltration into the porous medium (green) and the diffusion in the porous medium (white).

Table 1
Model parameters used for the simulations of the film and porous substrate model. ⋆ Van Genuchten parameter, ⋆⋆ Brooks and Corey parameter.

Parameter name	Symbol	Value
initial drop volume per length	$\mathcal{V}$	20.9 mm^2
liquid-gas interface energy	γ	70 mN.m^{-1}
water density	ρ	10^3 kg.m^{-3}
gravitational acceleration	g	9.81 m.s^{-2}
water viscosity ($T = 20\,°C$)	μ	10^{-3} Pa.s
water precursor layer height	ζ_p	20 μm
soil thickness	D	5 mm
soil porosity	ϕ	0.43
air compressibility	κ	200
macroscopic surface tension	Γ	1.7 mN
capillary height (of fine sand)	H_{cap}	26 cm
saturated hydraulic conductivity	K_{sat}	10^{-4} m.s^{-1}
pore size distribution coefficient⋆	n	3.31
pore size distribution coefficient⋆⋆	λ	0.972
imbibition rate coefficient	β	44 nm.Pa^{-1}.s^{-1}
simulation domain length	L	40 mm
repellent saturation	s_r	0.05
repellent range coefficient	σ	0.2
adaption substrate wetting	A	0.4
amplitude factor amplitude	ϑ	1.418 m
amplitude factor exponent	υ	1.402

where $\Omega = [-L, L]$ is the domain studied. Spatial gradient of the free energy is responsible to water flux. To model the time evolution of both variables, we adopt a gradient dynamics of the coupled kinetics of scalar fields (ζ, ξ) as described in Thiele [70] and developed for our context in Cajot [14].

In the next subsections, we describe the gradient dynamics in each medium: drop on a substrate (Section 2.2) and water in porous medium (Section 2.3) separately. Then, we present the coupled drop/porous medium energy (Section 2.4).

2.2. Drop on an impervious and initially dry substrate

In this section, we present the model of a thin liquid film on a flat impervious and dry substrate in the case of partial wetting. The dynamics of the thin film is based on a lubrication-type model, i.e. the flow is assumed to be quasi-static approximation with long wavelength hypothesis [61,72]. Although the description of the hydrodynamics is not strictly exact, the thermodynamic evolution of the system is faithfully reproduced. The thin film hydrodynamic models can be interpreted as gradient dynamics on underlying energy functional using Onsager principle [70]. In this context, the governing equation of the drop water height ζ is a gradient dynamics of ζ as a conserved order parameter field [58,63,70]:

$$\partial_t \zeta = \partial_x \left[Q(\zeta) \partial_x \frac{\delta \mathcal{F}^\zeta}{\delta \zeta} \right], \tag{4a}$$

$$\mathcal{F}^\zeta[\zeta] = \int_{-L}^{L} \left[\frac{\gamma}{2} |\partial_x \zeta|^2 + f_w^\zeta(\zeta) \right] \mathrm{d}x, \tag{4b}$$

The function $Q(\zeta)$ represents the mobility and it is equal to $\zeta^3/(3\mu)$ for a planar free surface flow with no-slip boundary condition, as considered in the present paper. The free energy $\mathcal{F}^\zeta$ of the system results from two terms: the free surface energy $f_\nabla^\zeta(\zeta) = |\partial_x \zeta|^2 \gamma/2$ related to the surface tension γ (supplementary Appendix B) and the wetting energy $f_w^\zeta(\zeta)$, also called the density wetting free energy, which takes into account the effective interaction between a solid surface and the water free surface [46]. Here, we neglect the variation of the gravity free energy compared to the two other free energy variations because, on one hand, it is small for the submillimetric droplets considered here and, on an other hand, we aim at focusing on the wettability effect.

The sandy porous medium considered here presents a high polarity [65]. Polar interaction is responsible for the complete wetting of the substrate and it is associated to hydrophilic interaction. In contrast, if amphiphilic matter is coating at sand grains, then polar interactions can be hindered by the long apolar tail of the amphiphilic molecules [32]. Due to surface tension, water dewets the substrate which is associated to a repellent-like behavior. In our case, wetting free energy should contain the polar and apolar interactions as commonly presented in the literature [29,8,7,71,38]. Resulting from these polar/apolar interactions, the wetting energy f_w^ζ can be represented as a sum of a long-range polar interaction f_{wpo}^ζ and a short-range apolar interaction f_{wap}^ζ as in [8,7]:

$$f_w^\zeta(\zeta, c) = f_{wpo}^\zeta(\zeta) + a_0(c) f_{wap}^\zeta(\zeta), \tag{5a}$$

$$f_{wpo}^\zeta(\zeta) = \frac{\Pi_0 b_0}{2} \frac{\zeta_p^3}{\zeta^2}, \tag{5b}$$

$$f_{wap}^\zeta(\zeta) = -\Pi_0 \zeta_p \exp\left(-\frac{\zeta}{\zeta_p} \right), \tag{5c}$$

where ζ_p is a precursor film of the drop and Π_0 is the dimensional parameter associates to the amplitude factor of the disjoining pressure. The dimensionless coefficients a_0 and b_0 are positive and modulate the polar and apolar terms, respectively. The amplitude b_0 of the long range polar interaction determines the wettability range. The effective interaction range of the porous medium surface has to match with the magnitude order of its roughness i.e. the grain size diameter. Throughout this paper, we assume a grain size diameter of 200 μm. We define the parameter $b_0 = \exp(-1) \approx 0.3679$ such that the effective interaction range is lower than 200 μm. Regarding the apolar interaction, we assume that only a_0 depends on the amphiphilic matter concentration. Because of the presence of apolar chains in the amphiphilic matter, coefficient a_0 is an increasing function of the concentration.

For vanishing height ζ, as long as $b_0 > 0$, the polar term f_{wpo}^ζ dominates. If $3b_0/a_0 > \exp(-1)$ then, a stable ultra-thin film $\zeta_p^\star$ exists such as $\partial f_w^\zeta/\partial\zeta(\zeta_p^\star) = 0$ and $\partial^2 f_w^\zeta/\partial\zeta^2(\zeta_p^\star) > 0$ [8,7]. The coexistence of this ultra-thin film with a thick film leads to a pseudo partial wetting where droplets may exist but the substrate is never totally dry. This ultra-thin refers initially to a precursor film of a few nanometers which is very quickly developed before a drop completely spread. In this modeling the precursor height ζ_p represents a cut-off scale but not necessarily a pseudo partial wetting. Note that ζ_p is small (20 μm) compared to the soil roughness (200 μm) which represents the magnitude order of the interaction range.

The variational derivative of the wetting free energy

$$\Pi(\zeta) = -\partial_\zeta f_w^\zeta = \Pi_0 \left[b_0 \left(\frac{\zeta_p}{\zeta} \right)^3 - a_0 \exp\left(-\frac{\zeta}{\zeta_p} \right) \right] \tag{6}$$

is the so-called disjoining pressure [36]. The function $\Pi(\zeta)$ represents the pressure due to the effective interaction between the free surface of the drop and the surface of the substrate.

From measurements and observations, the static contact angle of a drop on dry sand containing different concentrations is ranged from 10 to around 20 degrees. A quadratic dependence on the concentration c of parameter a_0 fits the experimental trend:

$$a_0(c) = A + (1 - A)c^2, \tag{7}$$

where A is the value a_0 of a drop on an impermeable dry substrate without amphiphilic matter. We estimate the contact angle of the drop on a dry substrate, such as sand grains without amphiphilic matter, to be about 10° from which we deduce $A = 0.4$ and fix this value throughout the paper.

2.3. Unsaturated porous medium

In this section, we consider an unsaturated porous layer of porosity ϕ with a mean vertical saturation over a thickness D and an equivalent height of water ξ defined in Eq. (1). Adapting the model for amphiphilic porous media recently developed in Cajot et al. [15], accounting for the variable ξ the governing equation of the water transfer in an amphiphilic porous medium can be written as a gradient model:

$$\partial_t \xi = D \partial_x \left[K(\xi) \partial_x \frac{\delta \mathcal{F}^\xi}{\delta \xi} \right], \tag{8a}$$

$$\mathcal{F}^\xi[\xi, c] = \int_{-L}^{L} \left[f_\nabla^\xi(\xi) + f_w^\xi(\xi, c) \right] \mathrm{d}x, \tag{8b}$$

where $K(\xi)$ is the hydraulic conductivity of the porous medium, which can be described by the van Genuchten-Mualem relationship [59,37]:

$$K(\xi) = \frac{K_{sat}}{\rho g} \sqrt{\frac{\xi}{\phi D}} \left[1 - \left(1 - \left(\frac{\xi}{\phi D} \right)^{\frac{1}{m}} \right)^m \right]^2, \tag{9}$$

with $m = 1 - 1/n$ and $n > 1$ is linked to the pore size distribution.

According to Beltrame and Cajot [6] the free energy is the sum of the wettability energy between water and porous matrix and the free surface energy of water in the porous medium, both of these being described below.

2.3.1. Water free surface energy in porous medium

The energy associated to the water/air interface in an unsaturated porous medium is usually neglected in literature. The energy associated to the water/air interface in an unsaturated porous medium is expressed as in Cueto-Felgueroso and Juanes works [23,25] (supplementary Appendix B):

$$f_\nabla^\xi(\xi) = \frac{\Gamma}{2\phi D} |\partial_x \xi|^2, \tag{10}$$

where Γ is called macroscopic surface tension [25]. Note that the expression of energy density due to the free surface is the same expression as for a thin film. However, Γ has not the same unit as the surface tension γ. Physically, free energy term f_∇^ξ represents the energy cost of creating the free surface of the water in porous medium [13]. This term is not only useful for improving the accuracy of the model, but also plays a decisive role in the consistency of the model in the case of hydrophobic interaction [6].

2.3.2. Wettability energy in porous medium

In Beltrame and Cajot [6], we generalized the capillary pressure by introducing a disjoining pressure for hydrophobic soil. As for impervious substrate, this wetting energy is a competition between attractive and repulsive interactions including air compression. The repellent interaction acts at low saturation while the attractive interaction acts at higher saturation, finally the air compression interaction acts close to the saturation.

The wettability density energy in the porous medium is the sum of three terms: capillary term f_c^ξ, repellent term f_r^ξ and the air compression term f_{comp}^ξ,

$$f_w^\xi(\xi, c) = f_c^\xi(\xi) + \chi(c) f_r^\xi(\xi) + f_{comp}^\xi(\xi), \tag{11}$$

where $\chi(c)$ is an amplitude factor depending on c the concentration of amphiphilic matter which increase the repellent energy with respect to c.

This amplitude factor $\chi(c)$ is a power law using an amplitude $\vartheta \geq 0$ and a constant exponent $\upsilon \geq 0$ to represent this amplitude factor,

$$\chi(c) = \frac{\vartheta}{H_{cap}} c^\upsilon, \tag{12}$$

with $\vartheta = 1.418$ m and $\upsilon = 1.402$ for EPS [14,15].

The capillary density energy can be described using the Brooks and Corey analytical expression [11,25],

$$f_c^\xi(\xi) = -\rho g H_{cap} \phi D \frac{\lambda}{\lambda - 1} \left(\frac{\xi}{\phi D} \right)^{1 - \frac{1}{\lambda}}, \tag{13}$$

with H_{cap} is the capillary height and $\lambda \neq 1$ is related to the pore size distribution in the soil.

The repellent density energy for EPS is given by

$$f_r^\xi(\xi) = 2\rho g H_{cap} \phi D \, \mathrm{erf}\left(\frac{\xi - \phi D s_r}{\phi D \sqrt{2} \sigma} \right), \tag{14}$$

where s_r is the repellent saturation ($s_r = 0.05$), σ is the dispersion coefficient ($\sigma = 0.2$) and erf is the error function [15].

The air compression density energy f_{comp}, defined by Cueto-Felgueroso and Juanes [24], writes

$$f_{comp}^\xi(\xi) = \mathrm{sgn}(\lambda - 1) \exp\left[-\kappa \left(1 - \frac{\xi}{\phi D} \right) \right] f_c^\xi(\xi), \tag{15}$$

where $\kappa \geq 0$ represents the air compression [25].

By analogy with the thin film (Section 2.2), the wettability density energy is related to the dimensionless disjoining pressure $\Pi_w(\xi)$,

$$\Pi_w(\xi, c) = -\frac{\partial_\xi f_w^\xi(\xi, c)}{\rho g H_{cap}}. \tag{16}$$

Using Eq. (1), the disjoining pressure can also be expressed as a function of the saturation. The use of saturation formulation highlights the bounded value of the water in the soil, while the use of height formulation is relevant to study the mass conservation between the two media.

2.4. Drop and porous medium coupled system

In this section, the coupling of the two previous models is developed for a drop deposited on a porous medium.

2.4.1. Drop and porous medium interface

Experiments in literature show that the drop spreading does not only depend on amphiphilic matter concentration but also on saturation [32,56]. The drop spreading is wider on wet than on dry porous medium. A common explanation is that the conformation of amphiphilic matter changes for wet porous medium. The apolar chain is then embedded in water, hiding the apolar chain of the molecules. We model this phenomenon by a linear decreasing of the apolar $f_{wap}^\zeta(\zeta)$ amplitude

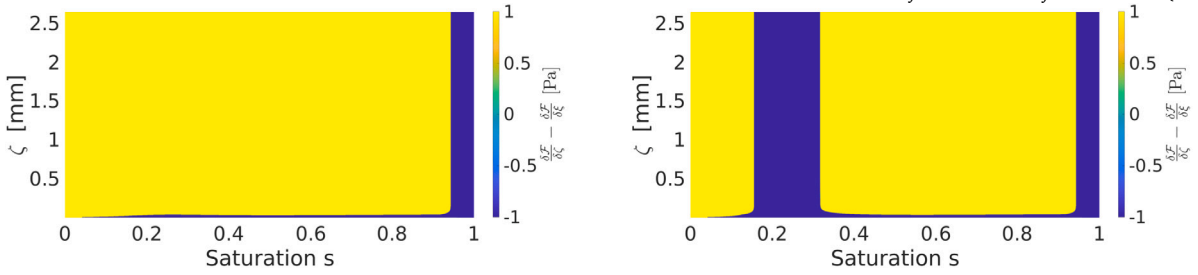

(a) $c = 0.6$ (b) $c = 0.8$

Fig. 2. Pressure difference $\delta\mathcal{F}/\delta\zeta - \delta\mathcal{F}/\delta\xi$ between liquid film and porous medium for homogeneous profiles as a function of saturation and water height. Parameters are given in Table 1 and other are $b = 0.3679$, $\Pi_0 = 9514$ Pa.

of the wetting drop energy as the saturation of the porous medium increases [7]. Therefore, the amplitude $a_0(c)$ in front of $f^{\zeta}_{wap}(\zeta)$ in Eq. (5a) becomes for coupled porous medium and water drop system

$$a(\xi, c) = a_0(c)\left(1 - \frac{\xi}{\phi D}\right), \tag{17}$$

and the wetting density energy is written as

$$f_w(\zeta, \xi, c) = f^{\zeta}_{wpo}(\zeta) + a(\xi, c) f^{\zeta}_{wap}(\zeta) + f^{\xi}_{w}(\xi, c). \tag{18}$$

This interaction can be interpreted as an additional interface energy between the bulk of the drop and of the porous medium such as

$$f_w(\zeta, \xi, c) = f^{\zeta}_{w}(\zeta, c) + f^{int}(\zeta, \xi, c) + f^{\xi}_{w}(\xi, c), \tag{19}$$

where

$$f^{int}(\zeta, \xi, c) = \big(a(\xi, c) - a_0(c)\big) f^{\zeta}_{wap}(\zeta). \tag{20}$$

According to the general decomposition of the free energy Eq. (3), we identify three free energy densities: drop on a dry substrate $f^{\zeta}(\zeta, c)$, wettability in the porous medium $f^{\xi}(\xi, c)$ and *interface energy* $f^{int}(\zeta, \xi, c)$ corresponding to an energy coupling term between the bulk of the drop and of the wet porous medium.

This interface energy modifies the pressure in the drop but also in the porous medium by adding $\delta\mathcal{F}^{int}/\delta\zeta$ and $\delta\mathcal{F}^{int}/\delta\xi$, respectively:

$$\frac{\delta\mathcal{F}^{int}}{\delta\zeta} = \big[a(\xi, c) - a_0(c)\big]\, \partial_\zeta f^{\zeta}_{wap}(\zeta), \tag{21a}$$

$$\frac{\delta\mathcal{F}^{int}}{\delta\xi} = \partial_\xi a(\xi, c) f^{\zeta}_{wap}(\zeta). \tag{21b}$$

The added pressure Eq. (21a) is a hydrophilic interaction since it is always negative. This indicates that wet porous medium is more hydrophilic than dry porous medium. In a similar way, the added pressure Eq. (21b) is always positive indicating that the porous medium is more hydrophobic when a very thin water film is present. Such an interaction between a thin film and the porous medium is not described in the porous medium literature. However, in polymer science, a similar interaction between drop and polymer brush is also derived from a free energy approach [71,40,38,48].

2.4.2. Exchange of water between drop and porous medium

In this section, water flux at the porous medium and drop interface is modeled. We assume the flux density, also called infiltration velocity, v of the drop into the porous medium proportional to the difference between the thin film and the porous medium pressure. As in the Washburn law in a porous medium [35], it reads:

$$v = \beta\left(\frac{\delta\mathcal{F}}{\delta\zeta} - \frac{\delta\mathcal{F}}{\delta\xi}\right) \tag{22}$$

where $\beta > 0$ is called transfer rate. Note that this expression of the infiltration velocity v is consistent with the dissipated free energy property [14].

Fig. 2 shows the difference between the thin film and the porous medium pressure for uniform (ζ, ξ) profiles. It represents the water flux sign when only the wetting energy is considered. The water infiltrates from the liquid film into the porous medium, if the pressure difference is positive (yellow area in Fig. 2). According to Fig. 2a, for $c = 0.6$, infiltration always occurs except for i) a saturation s greater than 0.94 or for ii) very small value of ζ. The first case corresponds to an almost saturated soil containing trapped air bubbles. The second case corresponds to a water film on the surface of the porous medium of the order of the precursor thickness ζ_p, that means to an almost dry surface.

For larger value of c, namely $c = 0.8$, a blue band appears for ξ between $s = 0.155$ and $s = 0.32$, impeding water infiltration (Fig. 2b). This band can be associated to an energy barrier due to the presence of hydrophobic terms in the wettability energies that we call 'hydrophobic barrier'. Water does not infiltrate spontaneously without an external free energy input.

2.4.3. Governing equations of the drop and porous medium coupled system

The free energy of the drop and porous medium coupled system is

$$\mathcal{F}[\zeta, \xi, c] = \int_\Omega \left[f^{\xi}_{\nabla}(\xi) + f^{\zeta}_{\nabla}(\zeta) + f^{\xi}_{w}(\xi, c) + f^{\zeta}_{w}(\zeta, c) + f^{int}(\zeta, \xi, c)\right] \mathrm{d}x. \tag{23}$$

The evolution of water in the drop-porous medium results from this energy, using the Onsager principle. The governing equation is derived from the drop dynamic [58,63,70], the water transfer in the porous medium [6] and the interface between the drop and the porous medium (Eq. (21a) and Eq. (21b)),

$$\partial_t \zeta = \partial_x\left[Q(\zeta)\partial_x \frac{\delta\mathcal{F}}{\delta\zeta}\right] - \beta\left(\frac{\delta\mathcal{F}}{\delta\zeta} - \frac{\delta\mathcal{F}}{\delta\xi}\right), \tag{24a}$$

$$\frac{\delta\mathcal{F}}{\delta\zeta} = \partial_\zeta f^{\zeta}_{w}(\zeta, c) + \partial_\zeta f^{int}(\zeta, \xi, c) - \gamma\partial_{xx}\zeta, \tag{24b}$$

$$\partial_t \xi = D\partial_x\left[K(\xi)\partial_x \frac{\delta\mathcal{F}}{\delta\xi}\right] + \beta\left(\frac{\delta\mathcal{F}}{\delta\zeta} - \frac{\delta\mathcal{F}}{\delta\xi}\right), \tag{24c}$$

$$\frac{\delta\mathcal{F}}{\delta\xi} = \partial_\xi f^{\xi}_{w}(\xi, c) + \partial_\xi f^{int}(\zeta, \xi, c) - T\partial_{xx}\xi, \tag{24d}$$

with $\delta\mathcal{F}/\delta\xi$ and $\delta\mathcal{F}/\delta\zeta$ are pressures in the bulk porous medium and at the drop surface, respectively.

The system of equations (24) represents the infiltration dynamics of a water film on a porous medium in the presence of amphiphilic matter. This model is partially parallels to model of drop on a polymer brush proposed by Thiele and Hartmann [71].

To solve the PDE system Eq. (24), we used a finite element approach using the C++ FEM library OOMPH-LIB [42]. For time-stepping, a backward differentiation formula (BDF) scheme of second order is used, while both the time-steps and the spatial mesh are adaptive to the dynamics.

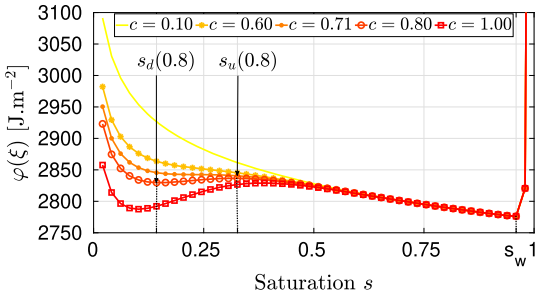

Fig. 3. Free density energy as a function of saturation s in the porous medium for different concentrations $c = \{0.1, 0.6, 0.71, 0.8, 1\}$ of amphiphilic EPS. Parameters are given in Table 1 and $H = \ell_c$ (2.65 mm).

3. Simulation results of water infiltration

3.1. Equilibria of flat film and uniform saturation

In this section, we study the different equilibria of the system (24) on the particular case of flat film and uniform saturation. This analysis is similar to the study of the sorption isotherm steady states of a brush [41].

3.1.1. Equilibrium and stability criterion

Assuming a uniform height of saturation ξ and a flat film ζ density free energy is equal to the wetting density energy, i.e. $f(\zeta, \xi, c) = f_w(\zeta, \xi, c)$. We note $U_0 = (\zeta_0, \xi_0)$ an equilibrium and for simplicity, we omit the dependence on c.

According to supplementary Appendix A, equilibrium implies pressure equilibrium and a zero flux v at the interface, namely:

$$\frac{\delta \mathcal{F}}{\delta \zeta}(U_0) - \frac{\delta \mathcal{F}}{\delta \xi}(U_0) = \frac{\partial f_w}{\partial \zeta}(U_0) - \frac{\partial f_w}{\partial \xi}(U_0) = 0. \tag{25}$$

Another equilibrium criterion can be established by introducing the total water height H which is proportional to the total water content:

$$H = \xi + \zeta. \tag{26}$$

Because of mass conservation, H is constant during infiltration. The wetting free energy can only expressed by the variable ξ:

$$\varphi(\xi) = f_w(\zeta(\xi), \xi), \tag{27}$$

where $\zeta(\xi) = H - \xi$ is the water film height. Then equilibria are extrema of the function φ (supplementary Appendix A). Furthermore, the equilibrium is stable at a local minimum of φ otherwise it is linearly unstable.

3.1.2. Equilibria with respect to H and c

We study the equilibria U_0 for a fine sandy soil with respect to the total amount H of water in the system. From the Eq. (27), we deduce uniform saturation s_0 and flat film ζ_0 for any couple (H, c) as shown in Section 3.1.

For instance, for a total water height equal to the capillary length $\ell_c \approx 2.65$ mm, three patterns emerge depending on concentration c:

i) $c < 0.71$ there is an unique global minimum reached when the medium is almost saturated, i.e. $s_w = 0.96$ (see curves with $c = 0.1$ and $c = 0.6$ in Fig. 3).
ii) $c \approx 0.71$ in addition to the global minimum corresponding to situation i), there is an inflection point in the dry zone around a saturation s_I (Fig. 3 - curve with $c = 0.71$).
iii) $c > 0.71$ in addition to the global minimum corresponding to situation i), there are two local extrema: a minimum in the dry zone around a saturation s_d and a maximum around a saturation s_u (Fig. 3 - curves with $c = 0.8$ and $c = 1.0$).

The critical concentration $c_{crit} \approx 0.71$ discriminates the i) and iii) water equilibria patterns, for any H.

For concentrations $c < c_{crit}$, corresponding to i), the unique equilibrium, called U_0^w, is the global minimum of the free energy $\mathcal{F}$. Therefore, water infiltrates in porous medium but for low height of water such as $H < \phi D$, there is not enough water to saturate the soil and the equilibrium saturation s_0 is inferior to $s_w \approx 0.96$ (Fig. 4b). Equilibrium saturation s_0 increases linearly as long as $H < \phi D$ while the equilibrium height ζ_0 remains almost zero (Fig. 4a). All equilibria for $c < c_{crit}$ seem to be the same. This can be explained by the fact that (i) the effect of the amphiphilic matter is negligible for these concentrations, and (ii) a final thin layer of water remains at soil surface, which the magnitude order is the precursor height ζ_p.

If $H > \phi D$, equilibrium saturation reaches saturation s_w and a thick layer ζ_0 of water remains, increasing linearly with H due to water that can no longer infiltrate.

When the concentration is greater than the critical concentration $c > c_{crit}$ (case iii), three possible equilibria may exist. In addition to U_0^w, there are two equilibria U_0^d (local minimum) and U_0^u (local maximum) associated respectively with the saturation s_d and s_u with $s_d < s_u$. Saturation s_d and s_u depend on concentration c. For $H = \ell_c$ and c increases from 0.80 to 1.0, the value of s_u increases from $s_u(0.8) = 0.317$ to $s_u(1) = 0.385$, whereas the value of s_d decreases from $s_d(0.8) = 0.151$ to $s_d(1) = 0.101$ (Fig. 3). Therefore, equilibrium U_0^d corresponds to a very dry porous medium coexisting under a non-infiltrated thick water layer and equilibrium saturation depends on the amphiphilic concentration but not on the height H (Fig. 4b). As U_0^u is an unstable equilibrium (Fig. 3), then two stable equilibria U_0^d and U_0^w may exist. Depending on the initial condition (saturation in the soil), the system converges to one of these stable equilibria. Since the free energy has to decrease during the dynamics then, there are three scenarios depending on the initial saturation s_i:

a) $s_i < s_d$: water slightly infiltrates to reach the equilibrium saturation s_d about 0.1
b) $s_d \leq s_i \leq s_u$: porous medium slightly dewets (negative velocity) until to converge to the equilibrium saturation s_d.
c) $s_i \geq s_u$: water infiltrates until to reach the saturation $s_w \approx 0.96$.

To conclude, this analysis shows that water may not infiltrate the porous medium if the concentration of amphiphilic EPS is sufficiently high and the porous medium sufficiently dry. Infiltration, until a saturation s_w is reached, occurs if the concentration is less than $c < c_{crit}$ (≈ 0.71 here) or if $s_i > s_u$ regardless of the concentration c. Otherwise, water almost does not infiltrate, or even flows out of the porous medium, with dry porous medium at saturation s_d which depends on c.

In the following, we do not only focus on uniform distribution of water over soil surface but on the infiltration of a drop in a fine sandy soil in presence of EPS. While the above equilibrium criterion provides some indications of the possibility of infiltration, numerical simulation is required to determine dynamics and the final equilibrium.

Note that stable equilibria are used to reproduce the initial soil profile before the drop is deposited.

3.2. Drop infiltration

In this section, we simulate the spreading and infiltration of a water drop on a fine sandy soil (grain size about 200 μm) containing amphiphilic EPS with a concentration c. The volume of water drop per unit length is fixed at 20.9 mm^2. The initial saturation of sandy soil and the EPS concentration c are the only parameters changing between each situation.

3.2.1. Initially wet porous medium

We consider a pre-wetted fine sandy soil with uniform saturation $s = 0.8$ and an EPS concentration $c = 0.8$ found in Section 3.1. We then

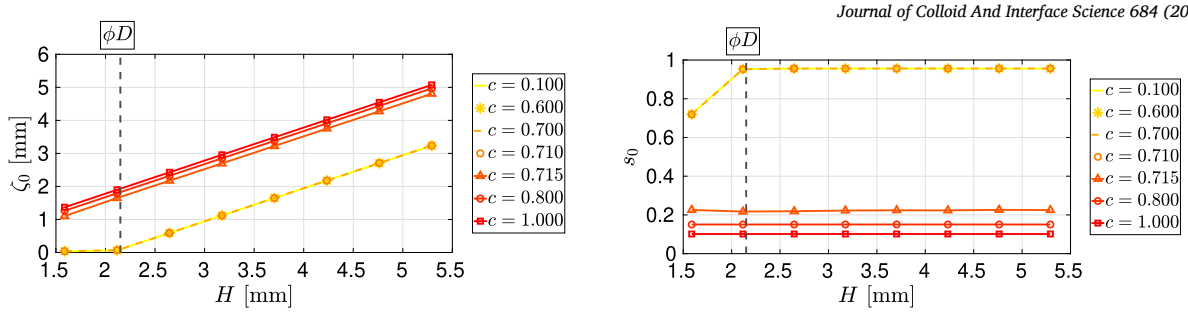

(a) Water film height ζ_0.

(b) Water saturation s_0.

Fig. 4. Equilibria (ζ_0, s_0) with respect to H for different concentrations c.

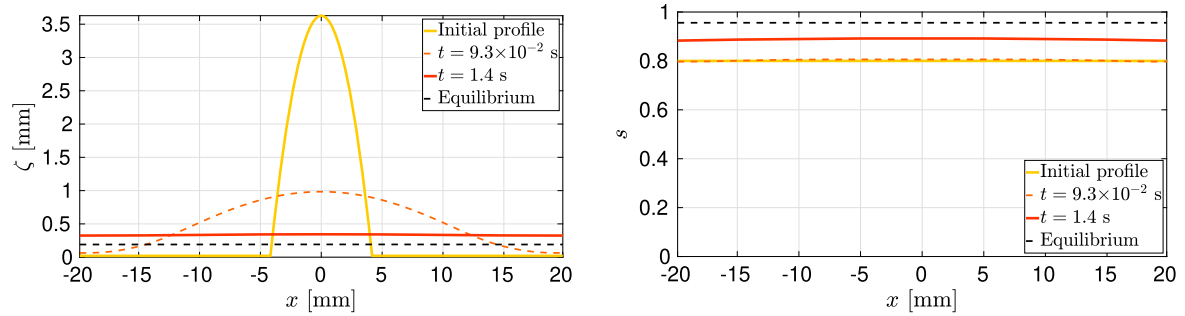

(a) Drop phase.

(b) Soil phase.

Fig. 5. Infiltration dynamic of a water drop, with a volume per unit length $\mathcal{V} = 20.9$ mm^2, in a wet soil ($s = 0.8$) and an EPS concentration $c = 0.8$. Parameters are given in Table 1.

place a 20.9 mm^2 drop on the surface and study its dynamics. Lateral boundary conditions are homogeneous Neumann conditions.

Fig. 5a shows the dynamics of the drop. It spreads rapidly over the substrate until reaching the domain boundaries (red arrows display in Fig. 1). This very fast dynamic takes about 0.1 s with negligible infiltration (as shown in Fig. 5 where saturation stays close to 0.8). The profile of the thin film of liquid is still drop-shaped: the drop height decreases from 3.5 to ≈ 1 mm. Because of the boundary conditions, the water no longer spreads out, but the profile gradually flattens out over the course of a second. At the same time, the water gradually percolates down (white arrows in Fig. 1). Then the saturation reaches at t about 3 s the compressibility barrier, ($s = s_w$). The dynamics converges to the same equilibrium computed in the Section 3.1.2 for the same total water height $H = 2.246$ mm.

A wet sandy soil without EPS ($c = 0$) and the same initial saturation behaves in a similar way, both qualitatively and quantitatively. As a result, soil moisture hides the effects of the amphiphilic matter, and the soil surface behaves like a substrate with complete wetting properties.

3.2.2. *Initially dry porous medium*

We consider the same drop and fine sandy soil as in Section 3.2.1 but the soil is dry with different EPS concentrations c. We fix the saturation in the porous medium at $s = 0.1$. This value corresponds to a dry medium for which the uniform profile is in a stable zone for $c \leq 1$ (Fig. 4). Equilibrium profiles of the liquid profiles of the water phase are displayed in Fig. 6. These profiles depend on concentration c.

As for a uniform water distribution, if $c < c_{crit}$ the drop infiltrates almost completely in the porous medium (Fig. 6a). A thin layer of water remains on the surface. The profile is not always uniform, being thicker where the drop has infiltrated (Fig. 6b). The infiltration criterion is the proportion of water infiltrated: if this remains below 12.6%, the drop is regarded to have completely infiltrated.

At low concentration ($c = 0.1$), the water infiltrates uniformly, whereas at higher concentration ($c \geq 0.6$ but inferior to c_{crit}), infiltration occurs essentially under the drop deposit. In the latter case, equilibrium water profile in the porous medium consists in a coexistence of dry and nearly saturated regions (Fig. 6b). This type of structure has been shown for hydrophobic soil in Beltrame and Cajot [6].

For $c > c_{crit}$, the drop fails to infiltrate. It is stopped by the hydrophobic barrier formed in the soil. For instance, the saturation at equilibrium for a concentration of $c = 0.8$ is about $s = 0.1$ corresponding to the hydrophobic barrier boundary in Fig. 2b.

Fig. 7 shows the time evolution of the drop volume for different concentrations of amphiphilic EPS. As expected, the total imbibition duration increases with the concentration c. Infiltration involves different stages associated with different infiltration rates. For concentration fairly lower than c_{crit}, there are two stages. During the first stage (≈ 1 s), the infiltration rate is maximal followed by a lower infiltration rate until total imbibition as shown Fig. 7 by the break in the slope of the infiltration curves, for $c = 0.1$ or $c = 0.6$.

For each stage, infiltration rate decreases with c. Approaching c_{crit}, the second stage of infiltration rate is nearly zero, between $t = 2$ and 14 s, for $c = 0.7$ (Fig. 7). Moreover, a third stage (between $t = 14$ and 23 s) appears with a higher infiltration rate followed by a fourth slower and last stage of infiltration until total imbibition. For concentration above c_{crit} infiltration stops after a short time (< 1 s). The equilibrium results in a drop remaining on porous medium. In this case, the infiltrated volume is negligible compared to the initial drop volume.

We detail in Fig. 8 the drop and saturation profiles for $c = 0.7$ at the different times stages. Initially, the drop spreads rapidly, $t = 10$ ms, over the substrate almost without infiltrating. Then, during the second stage, the radius of the drop decreases as it infiltrates vertically into the soil with little lateral diffusion. Infiltration is almost stopped as shown by the plateau of the infiltration curve in Fig. 7. This behavior is due to the hydrophobic barrier in the hydrophobic saturation range around $s = 0.12$ as shown in Fig. 8b. Once the hydrophobic saturation range has passed, infiltration is faster during the third and last stages. At the end of the last stage, the drop has infiltrated and the equilibrium state is reached after 35 s. There is a factor 1000 between the characteristic times of spreading and infiltration. In order to study in detail the

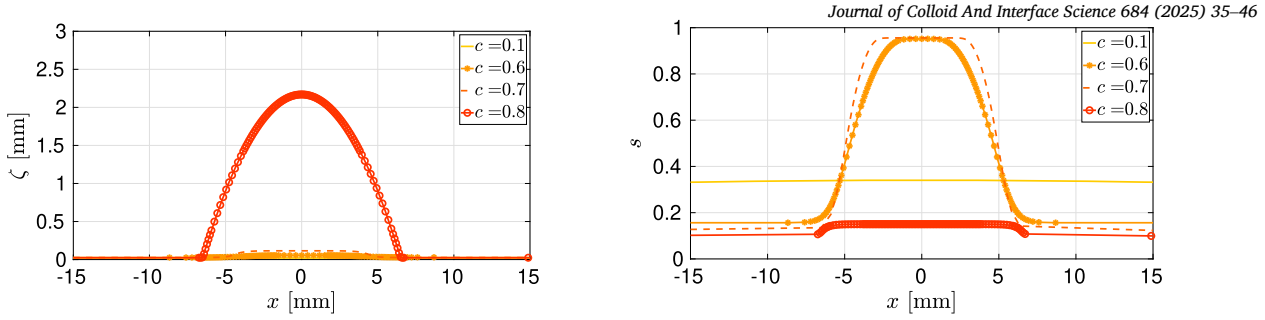

(a) Drop phase. (b) Soil phase.

Fig. 6. Equilibrium profiles of a drop on a dry sandy soil. Parameters are given in Table 1.

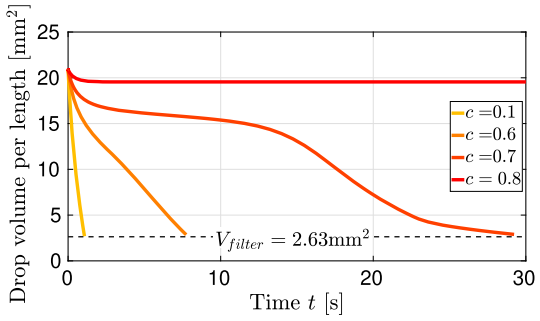

Fig. 7. Time evolution of drop volume per length during infiltration. The volume V_{filter} represented in black dashed line corresponds to 12.6% of the initial drop that imbibed into the sandy soil. This is the total infiltration criterion. Parameters are given in Table 1.

infiltration dynamics, we analyze the spreading radius of the drop, the evolution of the contact angle and the infiltration time.

In the literature, three infiltration stages were identified [57,28,44]:

i) Increasing Drawing Area (IDA): the radius of the drop increases while the angle decreases,
ii) Decreasing Drawing Area (DDA): the drop radius decreases and the contact angle remains constant,
iii) Constant Drawing Area (CDA): the drop radius remains constant (pinning of the contact line) and the contact angle decreases.

Fig. 9 represents the time evolution of drop radius and drop contact angle (logarithmic scale) to highlight the spreading dynamics. The numerical simulation of a soil with $c = 0.7$ displays the three stages dynamics described in literature while a soil with $c = 0.1$ and $c = 0.6$ display only the IDA and DDA dynamics (Fig. 9, $c = 0.1$ or $c = 0.6$).

In sand with $c = 0.1$, the IDA stage, corresponding to the spreading behavior lasts 0.14 second. During this stage, the contact angle decreases from 60° to 11° and the drop radius increases from 4.19 to 11 mm. After this spreading stage, the drop begins the DDA stage where the infiltration drives the dynamic, until total imbibition in the substrate after 6.6 seconds. During this stage, the contact angle decreases slightly until the equilibrium state corresponding to the complete imbibition.

From this study, the spreading times of the drop are lower than a millisecond for $c = 0.6$ and $c = 0.7$. It is relevant that these spreading times are shorter than for sand with a concentration of $c = 0.1$. We believe that the hydrophobicity at the interface drop/sand is the cause of this phenomenon, since it reduces the maximal drop radius. In contrast, the infiltration time into the substrate is shorter for low concentrations, going from 6.6 seconds for $c = 0.1$ to 35 seconds for $c = 0.7$.

These trends are consistent with the experimentally observed dynamics and our model is able to reproduce different experimental observations of infiltration dynamics in dry porous media.

3.2.3. Comparison with experiment

In this section, we present a qualitative validation of this model based on a comparison between the behavior of a drop during infiltration and experimental results. We simulate the infiltration of a second drop onto a medium previously wetted by a first drop. This experimental work corresponds to a qualitative experiment carried out in our laboratory to compare the infiltration dynamics of a drop on a dry and wet amphiphilic porous medium [14]. The experimental results are similar than those simulated previously. We consider a soil previously wet by a first drop of 20.9 mm^2. The initial saturation profile in soil corresponds to the equilibrium profile found in Section 3.2.2 after imbibition of the first drop on dry soil.

The infiltration behavior of the second drop is similar to the first: if the drop has not infiltrated, the second drop does not infiltrate, otherwise it infiltrates. Thus, for $c > 0.8$, the drop infiltrates slightly whereas for $c = 0.7$, it infiltrates almost completely.

At equilibrium, we distinguish two saturation profiles in the soil. For low concentration $c = 0.1$, the saturation profile is almost uniform whereas for higher concentration $c = 0.6$ and $c = 0.7$, the water is confined in the range $x \in [-10\text{ mm}, 10\text{ mm}]$. This equilibrium is qualitatively the same for the first drop deposit (Section 3.2.2), only the wetted portion of the soil is wider (Fig. 6). A similar behavior is pointed out in Beltrame and Cajot [6] when the mean water content is increased.

In contrast the infiltration dynamics differs between the first and the second deposit of the drop. Fig. 10b represents the time evolution of the drop volume per unit length of the first (line) and the second drop (dashed line). The curve associated to the second drop is convex, as described by Kumar and Deshpande [54]. Thus, for $c = 0.7$, only two stages of infiltration remain after the addition of a second drop: first the IDA stage followed by the DDA stage, while the CDA stage no longer exists.

This phenomenon was observed experimentally during the deposit of the second drop by Charles-Williams et al. [18] in the context of a powder medium without amphiphilic matter. As expected, the contact angle of the drop during infiltration is lower for pre-wetted soil than for dry soil (Fig. 10a). Comparing the time evolution of the drop volume per length between the first and second drop, the infiltration rate is faster for the second drop (Fig. 10b). However, after the infiltration plateau of the first deposit, the infiltration rate is higher than for the second deposit. As a result, the duration of imbibition is longer for the second drop ($t = 50$ s) than for the first drop on the dry substrate ($t = 35$ s).

Our model is able to reproduce both the infiltration time as well as the infiltration dynamics of the drop in a qualitative way between a dry soil and a wet soil.

4. Conclusions

We presented a model for the infiltration of a drop into a thin layer of porous medium containing adsorbed amphiphilic matter. The infiltration dynamic is interpreted as a relaxation dynamic. The resulting governing equations (24) which express the drop water heights ζ and the

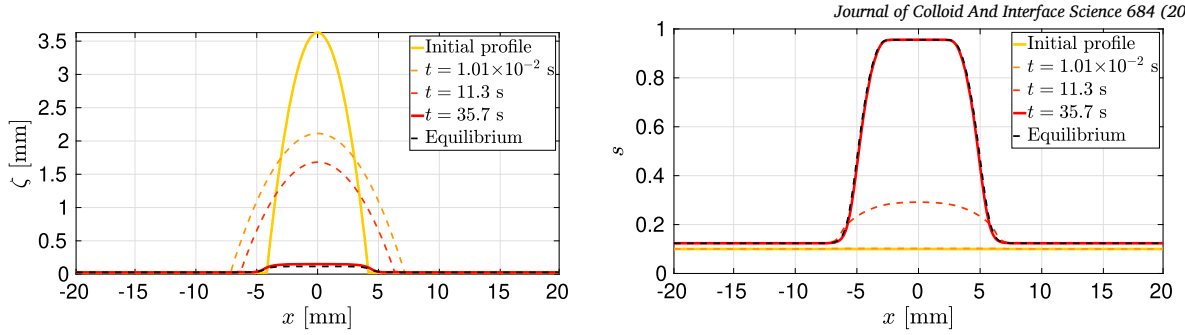

(a) Drop profil. (b) Saturation profile.

Fig. 8. Snapshots of height and saturation profiles during drop infiltration into a soil with EPS concentration $c = 0.7$. Initial drop volume per unit length is $\mathcal{V} = 20.9$ mm^2 and initial soil saturation is $s = 0.1$. Other parameters are given in Table 1.

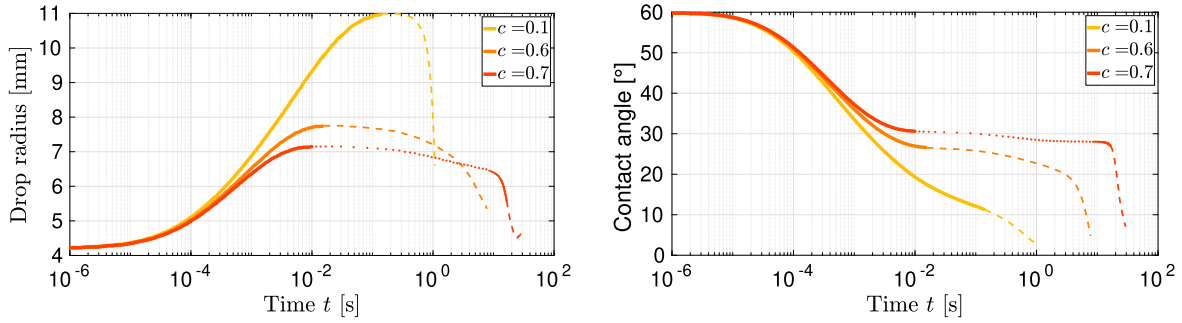

(a) Drop radius (b) Drop contact angle

Fig. 9. Time evolution (logarithmic scale) of (a) radius and (b) contact angle of a drop during infiltration into a dry sandy soil. [Line] Increasing Drawing Area (IDA), [Dashed] Decreasing Drawing Area (DDA) and [dotted] Constant Drawing Area (CDA). Parameters are given in Table 1.

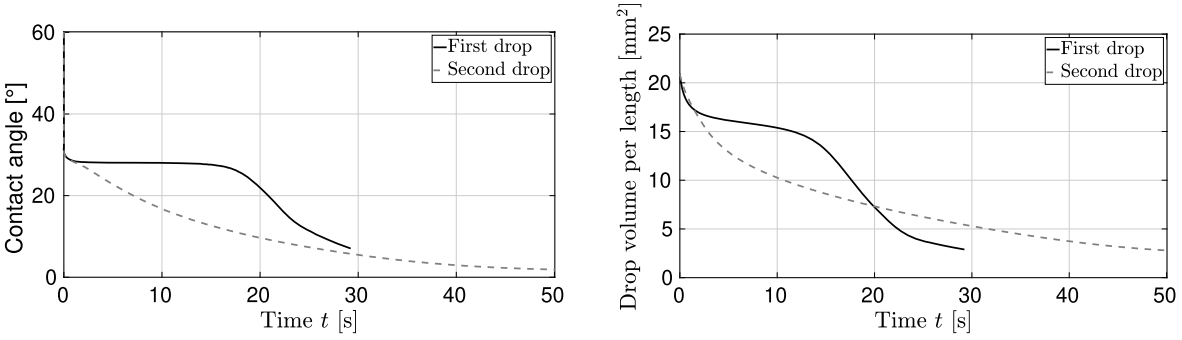

(a) Time evolution of drop contact angle. (b) Time evolution of drop volume (per unit length).

Fig. 10. Comparison of infiltration dynamics of a first drop deposit on a dry soil and of a second drop deposited at the same place, with soil wetted by the first drop (sandy soil with an amphiphilic EPS concentration $c = 0.7$). Parameters are given in Table 1.

equivalent height of saturation ξ in the medium are fourth-order nonlinear PDE belonging to the class of coupled (ζ, ξ) two-order-parameter gradient models [70]. We studied the uniform equilibria and their stability as well as the infiltration dynamics of a drop using a Finite Element Method code. The model mimics the dependence of the wettability of the porous medium and its interface on the amphiphilic matter and the water content. Numerical simulation demonstrates that the model is able to describe several dynamic processes for different situations which are driven by the same free functional energy. This energy includes (i) the surface tension at the wetting front in and on the porous medium [23,4] and (ii) the wettability of the amphiphilic porous medium [15], the drop [71,40] and at their interface, relevant to describe the water behavior during the infiltration into the porous medium. The emerging time processes of the model are the spreading of the drop, the vertical infiltration of liquid from the drop into the amphiphilic porous medium especially in dry substrate, the lateral diffusion of the liquid within the wet porous layer, and the delay of infiltration in dry porous medium depending on the concentration of amphiphilic matter.

The wettability within the porous medium and at its interface is a relevant notion for understanding processes and modeling water transfer with a functional free energy. In this way, the drop infiltration into a porous medium is described by a gradient model constructed from a free energy that combines the drop energy, the porous medium energy and coupled interface energy. This partial differential equation ensures consistency with thermodynamics, as in generic models of the coupled kinetics of scalar fields [70]. In this study, (i) we have adapted and extended models for amphiphilic porous medium by taking into account the wettability at the interface depending on the saturation and the drop height, (ii) we assume a quasistatic flow dynamic, we have neglected (iii) the viscous coupling of tangential velocity at the interface between

the liquid film and the thin porous medium and (iv) liquid evaporation.

Numerical simulation demonstrates a slowdown of infiltration in dry media similar to the slowdown of diffusion in rhizospheric soils [16,53] that has been interpreted as a decrease in hydraulic conductivity [52]. In contrast, in our study, this slowdown process spontaneously emerges from the wettability properties of the porous medium. More, our model results reveal an infiltration threshold, which cannot be explained by a variation in hydraulic conductivity. Slightly below this threshold value, an imbibition latency effect precedes drop infiltration due to the hydrophobicity of the medium. This phenomenon is observed in a natural media. The video in the supplementary material shows the imbibition dynamics of a drop in soil under a pine tree and therefore containing organic matter. A latency period is clearly visible. To our knowledge, current models in the literature do not reproduce this type of infiltration dynamics, despite their existence in natural media. However, the infiltration threshold is reminiscent of the depinning of a drop passing through a hydrophobic defect [7], or the infiltration threshold in a hydrophobic layer in stratified porous medium [6]. In all of these studies, the liquid must overcome an energy barrier related to hydrophobicity to continue flowing. To clearly identify this threshold would require a bifurcation study as conducted in [7].

The employed gradient dynamics approach provides a simple thermodynamics construction to model complex situations [70,40,41,30]. Here it has been restricted to fine porous media, notably to avoid the two-dimensional mesh of the porous medium. This case is relevant to model the infiltration of drops on paper [21] or on powder medium [39,18], as well as the transfer of water in a fine medium such as a Gas Diffusion Layer [1]. Extending this model to several dimensions (2 or 3) does not raise theoretical problems. However, taking into account the thickness of the porous medium requires coupling a two-dimensional mesh (inside the porous medium) and a one-dimensional mesh (drop/porous medium interface). This model can be applied and extended to practical problems in industry and natural as rehumectation and root uptake processes in the rhizosphere [16,53,55,14], flow phenomena on dry soil from run-off to infiltration [43,66], solutions on porous substrates [68,44], transport in mesoporous silica films [49]. Furthermore, the approach could be expanded to free amphiphilic matter in a solute or to liquid evaporation processes [73,22,31] by combining the gradient dynamics approach presented here with elements of polymer brush framework [71,40].

CRediT authorship contribution statement

Florian Cajot: Writing – original draft, Visualization, Validation, Software, Methodology, Investigation, Formal analysis, Conceptualization. **Claude Doussan:** Writing – review & editing, Supervision, Funding acquisition. **Simon Hartmann:** Software. **Philippe Beltrame:** Writing – review & editing, Writing – original draft, Validation, Supervision, Project administration, Methodology, Investigation, Funding acquisition, Conceptualization.

Declaration of competing interest

The authors declare that they have no known competing financial interests or personal relationships that could have appeared to influence the work reported in this paper.

Acknowledgement

The authors acknowledge support by INRAE and Avignon University which provided the PhD grant of FC. FC and PB acknowledge fruitful discussions with Uwe Thiele and greatly appreciate his valuable advices, aided by a Perdiguier program awarded to FC by Avignon Université. The authors thank Annette Bérard, Clémentine Lapie, Léo Corridor, Emy Garcia and Arnaud Chapelet for technical assistance and help in the design of experiments of drop infiltration in an amphiphilic sandy medium. PB further extends gratitude to Clara Bottalico for her experimental contribution and the resulting video of supplementary material.

Appendix. Supplementary material

Supplementary material related to this article can be found online at https://doi.org/10.1016/j.jcis.2024.12.216.

Data availability

Data will be made available on request.

References

[1] N. Abbaspour, Numerical and Experimental Approach for Bipolar Plates in PEM Fuel Cells: Novel Designs of Fluid Domain, PhD Thesis, Avignon Université, 2020.
[2] N. Abbaspour, P. Beltrame, M.C. Néel, V.P. Schulz, Directional water wicking on a metal surface patterned by microchannels, Materials 14 (3) (2021) 490, https://doi.org/10.3390/ma14030490, https://www.mdpi.com/1996-1944/14/3/490, Multidisciplinary Digital Publishing Institute.
[3] M.A. Ahmed, M. Holz, S.K. Woche, J. Bachmann, A. Carminati, Effect of soil drying on mucilage exudation and its water repellency: a new method to collect mucilage, J. Plant Nutr. Soil Sci. 178 (2015) 821–824, https://doi.org/10.1002/jpln.201500177, https://onlinelibrary.wiley.com/doi/abs/10.1002/jpln.201500177, https://onlinelibrary.wiley.com/doi/pdf/10.1002/jpln.201500177.
[4] A. Beljadid, L. Cueto-Felgueroso, R. Juanes, A continuum model of unstable infiltration in porous media endowed with an entropy function, Adv. Water Resour. 144 (2020) 103684, https://doi.org/10.1016/j.advwatres.2020.103684, https://linkinghub.elsevier.com/retrieve/pii/S0309170819308954.
[5] P. Beltrame, Drop train flow in a microtube, Eur. Phys. J. Spec. Top. 232 (2023) 435–442, https://doi.org/10.1140/epjs/s11734-023-00786-9.
[6] P. Beltrame, F. Cajot, Model of hydrophobic porous media applied to stratified media: water trapping, intermittent flow and fingering instability, Europhys. Lett. 138 (2022) 53004, https://doi.org/10.1209/0295-5075/ac71c1, https://dx.doi.org/10.1209/0295-5075/ac71c1, EDP Sciences, IOP Publishing and Società Italiana di Fisica.
[7] P. Beltrame, E. Knobloch, P. Hänggi, U. Thiele, Rayleigh and depinning instabilities of forced liquid ridges on heterogeneous substrates, Phys. Rev. E 83 (2011) 016305, https://doi.org/10.1103/PhysRevE.83.016305, https://link.aps.org/doi/10.1103/PhysRevE.83.016305, American Physical Society.
[8] P. Beltrame, U. Thiele, Time integration and steady-state continuation for 2d lubrication equations, SIAM J. Appl. Dyn. Syst. 9 (2010) 484–518, https://doi.org/10.1137/080718619, https://epubs.siam.org/doi/abs/10.1137/080718619, Society for Industrial and Applied Mathematics.
[9] P. Benard, M. Zarebanadkouki, A. Carminati, Impact of pore-scale wettability on rhizosphere rewetting, Front. Environ. Sci. 6 (2018), https://doi.org/10.3389/fenvs.2018.00016, https://www.frontiersin.org/articles/10.3389/fenvs.2018.00016, Frontiers.
[10] S. Biswas, P. Fantinel, O. Borgman, R. Holtzman, L. Goehring, Drying and percolation in correlated porous media, Phys. Rev. Fluids 3 (2018) 124307, https://doi.org/10.1103/PhysRevFluids.3.124307, https://link.aps.org/doi/10.1103/PhysRevFluids.3.124307, American Physical Society.
[11] R.H. Brooks, A.T. Corey, Properties of porous media affecting fluid flow, J. Irrig. Drain. Div. 92 (1966) 61–88, https://doi.org/10.1061/JRCEA4.0000425, https://ascelibrary.org/doi/10.1061/JRCEA4.0000425, American Society of Civil Engineers.
[12] A. Bérard, T. Clavel, C. Le Bourvellec, A. Davoine, S. Le Gall, C. Doussan, S. Bureau, Exopolysaccharides in the rhizosphere: a comparative study of extraction methods. Application to their quantification in Mediterranean soils, Soil Biol. Biochem. 149 (2020) 107961, https://doi.org/10.1016/j.soilbio.2020.107961, https://www.sciencedirect.com/science/article/pii/S0038071720302571.
[13] J.W. Cahn, J.E. Hilliard, Free energy of a nonuniform system. I. Interfacial free energy, J. Chem. Phys. 28 (2004) 258–267, https://doi.org/10.1063/1.1744102.
[14] F. Cajot, Modeling water transfer in soil in the presence of amphiphilic matter: application to the rhizosphere, These de doctorat, Avignon, 2024.
[15] F. Cajot, C. Doussan, P. Beltrame, A Free Energy Based Model for Water Transfer in Amphiphilic Soils, 2024, https://www.ssrn.com/abstract=4996972.
[16] A. Carminati, A.B. Moradi, D. Vetterlein, P. Vontobel, E. Lehmann, U. Weller, H.J. Vogel, S.E. Oswald, Dynamics of soil water content in the rhizosphere, Plant Soil 332 (2010) 163–176, https://doi.org/10.1007/s11104-010-0283-8, http://link.springer.com/10.1007/s11104-010-0283-8.
[17] K.Y. Chan, Development of seasonal water repellence under direct drilling, Soil Sci. Soc. Am. J. 56 (1992) 326–329, https://doi.org/10.2136/sssaj1992.03615995005600010054x, https://onlinelibrary.wiley.com/doi/abs/10.2136/sssaj1992.03615995005600010054x, https://onlinelibrary.wiley.com/doi/pdf/10.2136/sssaj1992.03615995005600010054x.

[18] H.R. Charles-Williams, R. Wengeler, K. Flore, H. Feise, M.J. Hounslow, A.D. Salman, Granule nucleation and growth: competing drop spreading and infiltration processes, Powder Technol. 206 (2011) 63–71, https://doi.org/10.1016/j.powtec.2010.06.013, https://www.sciencedirect.com/science/article/pii/S0032591010003128.

[19] C. Chenu, Y. Le Bissonnais, D. Arrouays, Organic matter influence on clay wettability and soil aggregate stability, Soil Sci. Soc. Am. J. 64 (2000) 1479–1486, https://doi.org/10.2136/sssaj2000.6441479x, https://onlinelibrary.wiley.com/doi/abs/10.2136/sssaj2000.6441479x, https://onlinelibrary.wiley.com/doi/pdf/10.2136/sssaj2000.6441479x.

[20] H. Choi, H. Liang, Wettability and spontaneous penetration of a water drop into hydrophobic pores, J. Colloid Interface Sci. 477 (2016) 176–180, https://doi.org/10.1016/j.jcis.2016.05.029, https://www.sciencedirect.com/science/article/pii/S0021979716303149.

[21] A. Clarke, T.D. Blake, K. Carruthers, A. Woodward, Spreading and imbibition of liquid droplets on porous surfaces, Langmuir 18 (2002) 2980–2984, https://doi.org/10.1021/la0117810, American Chemical Society.

[22] H. Crockford, S. Topalidis, D.P. Richardson, Water repellency in a dry sclerophyll eucalypt forest — measurements and processes, Hydrol. Process. 5 (1991) 405–420, https://doi.org/10.1002/hyp.3360050408, https://onlinelibrary.wiley.com/doi/abs/10.1002/hyp.3360050408, https://onlinelibrary.wiley.com/doi/pdf/10.1002/hyp.3360050408.

[23] L. Cueto-Felgueroso, R. Juanes, Nonlocal interface dynamics and pattern formation in gravity-driven unsaturated flow through porous media, Phys. Rev. Lett. 101 (2008) 244504, https://doi.org/10.1103/PhysRevLett.101.244504, https://link.aps.org/doi/10.1103/PhysRevLett.101.2, American Physical Society.

[24] L. Cueto-Felgueroso, R. Juanes, Adaptive rational spectral methods for the linear stability analysis of nonlinear fourth-order problems, J. Comput. Phys. 228 (2009) 6536–6552, https://doi.org/10.1016/j.jcp.2009.05.045, https://linkinghub.elsevier.com/retrieve/pii/S0021999109003179.

[25] L. Cueto-Felgueroso, R. Juanes, A phase field model of unsaturated flow, Water Resour. Res. 45 (2009), https://doi.org/10.1029/2009WR007945, https://onlinelibrary.wiley.com/doi/abs/10.1029/2009WR007945, https://onlinelibrary.wiley.com/doi/pdf/10.1029/2009WR007945.

[26] R.C. Daniel, J.C. Berg, Spreading on and penetration into thin, permeable print media: application to ink-jet printing, Adv. Colloid Interface Sci. 123–126 (2006) 439–469, https://doi.org/10.1016/j.cis.2006.05.012, https://www.sciencedirect.com/science/article/pii/S0001868606000637.

[27] L.W. Dekker, S.H. Doerr, K. Oostindie, A.K. Ziogas, C.J. Ritsema, Water repellency and critical soil water content in a dune sand, Soil Sci. Soc. Am. J. 65 (2001) 1667–1674, https://doi.org/10.2136/sssaj2001.1667, https://onlinelibrary.wiley.com/doi/abs/10.2136/sssaj2001.1667, https://onlinelibrary.wiley.com/doi/pdf/10.2136/sssaj2001.1667.

[28] M. Denesuk, G.L. Smith, B.J.J. Zelinski, N.J. Kreidl, D.R. Uhlmann, Capillary penetration of liquid droplets into porous materials, J. Colloid Interface Sci. 158 (1993) 114–120, https://doi.org/10.1006/jcis.1993.1235, https://www.sciencedirect.com/science/article/pii/S002197978371235X.

[29] B.V. Derjaguin, N.V. Churaev, V.M. Muller, Surface Forces, Springer US, Boston, MA, 1987, http://link.springer.com/10.1007/978-1-4757-6639-4.

[30] J. Diekmann, U. Thiele, Drops of volatile binary mixtures on brush-covered substrates, Eur. Phys. J. Spec. Top. (2024), https://doi.org/10.1140/epjs/s11734-024-01169-4.

[31] S.H. Doerr, On standardizing the 'water drop penetration time' and the 'molarity of an ethanol droplet' techniques to classify soil hydrophobicity: a case study using medium textured soils, Earth Surf. Process. Landf. 23 (1998) 663–668, https://doi.org/10.1002/(SICI)1096-9837(199807)23:7<663::AID-ESP909>3.0.CO;2-6, https://onlinelibrary.wiley.com/doi/abs/10.1002/%28SICI%291096-9837%28199807%2923%3A7%3C663%3A%3AAID-ESP909%3E3.0.CO%3B2-6, https://onlinelibrary.wiley.com/doi/pdf/10.1002/%28SICI%291096-9837%28199807%2923%3A7%3C663%3A%3AAID-ESP909%3E3.0.CO%3B2-6.

[32] S.H. Doerr, R.A. Shakesby, R.P.D. Walsh, Soil water repellency: its causes, characteristics and hydro-geomorphological significance, Earth-Sci. Rev. 51 (2000) 33–65, https://doi.org/10.1016/S0012-8252(00)00011-8, https://www.sciencedirect.com/science/article/pii/S0012825200000118.

[33] M. Doi, Onsager's variational principle in soft matter, J. Phys. Condens. Matter 23 (2011) 284118, https://doi.org/10.1088/0953-8984/23/28/284118, https://dx.doi.org/10.1088/0953-8984/23/28/284118.

[34] D.S. Feeney, P.D. Hallett, S. Rodger, A.G. Bengough, N.A. White, I.M. Young, Impact of fungal and bacterial biocides on microbial induced water repellency in arable soil, Geoderma 135 (2006) 72–80, https://doi.org/10.1016/j.geoderma.2005.11.007, https://www.sciencedirect.com/science/article/pii/S0016706105003022.

[35] T. Gambaryan-Roisman, Liquids on porous layers: wetting, imbibition and transport processes, Curr. Opin. Colloid Interface Sci. 19 (2014) 320–335, https://doi.org/10.1016/j.cocis.2014.09.001, https://www.sciencedirect.com/science/article/pii/S1359029414000880.

[36] P.G. de Gennes, Wetting: statics and dynamics, Rev. Mod. Phys. 57 (1985) 827–863, https://doi.org/10.1103/RevModPhys.57.827, https://link.aps.org/doi/10.1103/RevModPhys.57.827, American Physical Society.

[37] M.T. van Genuchten, A closed-form equation for predicting the hydraulic conductivity of unsaturated soils, Soil Sci. Soc. Am. J. 44 (1980) 892–898, https://doi.org/10.2136/sssaj1980.03615995004400050002x, https://onlinelibrary.wiley.com/doi/abs/10.2136/sssaj1980.03615995004400050002x, https://onlinelibrary.wiley.com/doi/pdf/10.2136/sssaj1980.03615995004400050002x.

[38] D. Greve, S. Hartmann, U. Thiele, Stick-slip dynamics in the forced wetting of polymer brushes, Soft Matter (2023), https://doi.org/10.1039/D3SM00104K, https://pubs.rsc.org/en/content/articlelanding/2023/sm/d3sm00104k, The Royal Society of Chemistry.

[39] K.P. Hapgood, J.D. Litster, S.R. Biggs, T. Howes, Drop penetration into porous powder beds, J. Colloid Interface Sci. 253 (2002) 353–366, https://doi.org/10.1006/jcis.2002.8527, https://linkinghub.elsevier.com/retrieve/pii/S0021979702985279.

[40] S. Hartmann, C. Diddens, M. Jalaal, U. Thiele, Sessile drop evaporation in a gap – crossover between diffusion-limited and phase transition-limited regime, J. Fluid Mech. 960 (2023) A32, https://doi.org/10.1017/jfm.2023.176, https://www.cambridge.org/core/journals/journal-of-fluid-mechanics/article/sessile-drop-evaporation-in-a-gap-crossover-between-diffusionlimited-and-phase-transitionlimited-regime/3F1AB5923526F5E6714F3C1953894D92, Cambridge University Press.

[41] S. Hartmann, J. Diekmann, D. Greve, U. Thiele, Drops on polymer brushes: advances in thin-film modeling of adaptive substrates, Langmuir 40 (2024) 4001–4021, https://doi.org/10.1021/acs.langmuir.3c03313, American Chemical Society.

[42] M. Heil, A.L. Hazel, Oomph-lib – an object-oriented multi-physics finite-element library, in: H.J. Bungartz, M. Schäfer (Eds.), Fluid-Structure Interaction, Springer, Berlin, Heidelberg, 2006, pp. 19–49.

[43] D.E. Hill, J.Y. Parlange, Wetting front instability in layered soils, Soil Sci. Soc. Am. J. 36 (1972) 697–702, https://doi.org/10.2136/sssaj1972.03615995003600050010x, https://onlinelibrary.wiley.com/doi/abs/10.2136/sssaj1972.03615995003600050010x, https://onlinelibrary.wiley.com/doi/pdf/10.2136/sssaj1972.03615995003600050010x.

[44] R.K. Holman, M.J. Cima, S.A. Uhland, E. Sachs, Spreading and infiltration of inkjet-printed polymer solution droplets on a porous substrate, J. Colloid Interface Sci. 249 (2002) 432–440, https://doi.org/10.1006/jcis.2002.8225, https://www.sciencedirect.com/science/article/pii/S0021979702982251.

[45] R. Holtzman, E. Segre, Wettability stabilizes fluid invasion into porous media via nonlocal, cooperative pore filling, Phys. Rev. Lett. 115 (2015) 164501, https://doi.org/10.1103/PhysRevLett.115.164501, https://link.aps.org/doi/10.1103/PhysRevLett.115.164501, American Physical Society.

[46] J.N. Israelachvili, Forces between surfaces in liquids, Adv. Colloid Interface Sci. 16 (1982) 31–47, https://doi.org/10.1016/0001-8686(82)85004-5, https://www.sciencedirect.com/science/article/pii/0001868682850045.

[47] H. Kang, S.D.N. Lourenço, W.M. Yan, Lattice Boltzmann simulation of droplet dynamics on granular surfaces with variable wettability, Phys. Rev. E 98 (2018) 012902, https://doi.org/10.1103/PhysRevE.98.012902, https://link.aps.org/doi/10.1103/PhysRevE.98.012902, American Physical Society.

[48] O. Kap, S. Hartmann, H. Hoek, S. de Beer, I. Siretanu, U. Thiele, F. Mugele, Nonequilibrium configurations of swelling polymer brush layers induced by spreading drops of weakly volatile oil, J. Chem. Phys. 158 (2023) 174903, https://doi.org/10.1063/5.0146779.

[49] A. Khalil, M. Zimmermann, A.K. Bell, U. Kunz, S. Hardt, H.J. Kleebe, R.W. Stark, P. Stephan, A. Andrieu-Brunsen, Insights into the interplay of wetting and transport in mesoporous silica films, J. Colloid Interface Sci. 560 (2020) 369–378, https://doi.org/10.1016/j.jcis.2019.09.093, https://www.sciencedirect.com/science/article/pii/S0021979719311361.

[50] M. Knott, M. Ani, E. Kroener, D. Diehl, Effect of changing chemical environment on physical properties of maize root mucilage, Plant Soil 478 (2022) 85–101, https://doi.org/10.1007/s11104-022-05577-0.

[51] E. Kroener, Roots at the percolation threshold, Phys. Rev. E 91 (2015), https://doi.org/10.1103/PhysRevE.91.042706.

[52] E. Kroener, M. Holz, M. Zarebanadkouki, M. Ahmed, A. Carminati, Effects of mucilage on rhizosphere hydraulic functions depend on soil particle size, Vadose Zone J. 17 (2018) 170056, https://doi.org/10.2136/vzj2017.03.0056, https://onlinelibrary.wiley.com/doi/abs/10.2136/vzj2017.03.0056, https://onlinelibrary.wiley.com/doi/pdf/10.2136/vzj2017.03.0056.

[53] E. Kroener, M. Zarebanadkouki, A. Kaestner, A. Carminati, Nonequilibrium water dynamics in the rhizosphere: how mucilage affects water flow in soils, Water Resour. Res. 50 (2014) 6479–6495, https://doi.org/10.1002/2013WR014756, https://onlinelibrary.wiley.com/doi/abs/10.1002/2013WR014756, https://onlinelibrary.wiley.com/doi/pdf/10.1002/2013WR014756.

[54] S.M. Kumar, A.P. Deshpande, Dynamics of drop spreading on fibrous porous media, Colloids Surf. A, Physicochem. Eng. Asp. 277 (2006) 157–163, https://doi.org/10.1016/j.colsurfa.2005.11.056, https://www.sciencedirect.com/science/article/pii/S0927775705009003.

[55] M. Landl, M. Phalempin, S. Schlüter, D. Vetterlein, J. Vanderborght, E. Kroener, A. Schnepf, Modeling the impact of rhizosphere bulk density and mucilage gradients on root water uptake, Front. Agron. 3 (2021), https://www.frontiersin.org/articles/10.3389/fagro.2021.622367.

[56] H. Liu, Z. Ju, J. Bachmann, R. Horton, T. Ren, Moisture-dependent wettability of artificial hydrophobic soils and its relevance for soil water desorption curves, Soil Sci. Soc. Am. J. 76 (2012) 342–349, https://doi.org/10.2136/sssaj2011.0081, https://onlinelibrary.wiley.com/doi/abs/10.2136/sssaj2011.0081, https://onlinelibrary.wiley.com/doi/pdf/10.2136/sssaj2011.0081.

[57] A. Marmur, Drop penetration into a thin porous medium, J. Colloid Interface Sci. 123 (1988) 161–169, https://doi.org/10.1016/0021-9797(88)90233-0, https://www.sciencedirect.com/science/article/pii/0021979788902330.

[58] V.S. Mitlin, Dewetting of solid surface: analogy with spinodal decomposition, J. Colloid Interface Sci. 156 (1993) 491–497, https://doi.org/10.1006/jcis.1993.1142, https://www.sciencedirect.com/science/article/pii/S0021979783711422.

[59] Y. Mualem, A new model for predicting the hydraulic conductivity of unsaturated porous media, Water Resour. Res. 12 (1976) 513–522, https://doi.org/10.1029/WR012i003p00513, https://onlinelibrary.wiley.com/doi/abs/10.1029/WR012i003p00513, https://onlinelibrary.wiley.com/doi/pdf/10.1029/WR012i003p00513.

[60] T. Orfánus, A. Zvala, M. Čierniková, D. Stojkovová, V. Nagy, P. Dlapa, Peculiarities of infiltration measurements in water-repellent forest soil, Forests 12 (2021) 472, https://doi.org/10.3390/f12040472, https://www.mdpi.com/1999-4907/12/4/472, Multidisciplinary Digital Publishing Institute.

[61] A. Oron, S.H. Davis, S.G. Bankoff, Long-scale evolution of thin liquid films, Rev. Mod. Phys. 69 (1997) 931–980, https://doi.org/10.1103/RevModPhys.69.931, https://link.aps.org/doi/10.1103/RevModPhys.69.931, American Physical Society.

[62] X. Pepin, S. Blanchon, G. Couarraze, Powder dynamic contact angle measurements: young contact angles and effectively wet perimeters, Powder Technol. 99 (1998) 264–271, https://doi.org/10.1016/S0032-5910(98)00123-5, https://www.sciencedirect.com/science/article/pii/S0032591098001235.

[63] L.M. Pismen, Y. Pomeau, Disjoining potential and spreading of thin liquid layers in the diffuse-interface model coupled to hydrodynamics, Phys. Rev. E 62 (2000) 2480–2492, https://doi.org/10.1103/PhysRevE.62.2480, https://link.aps.org/doi/10.1103/PhysRevE.62.2480, American Physical Society.

[64] L.A. Richards, Capillary conduction of liquids through porous mediums, Physics 1 (1931) 318–333, https://doi.org/10.1063/1.1745010, http://aip.scitation.org/doi/10.1063/1.1745010.

[65] J. Sagiv, Organized monolayers by adsorption. 1. Formation and structure of oleophobic mixed monolayers on solid surfaces, J. Am. Chem. Soc. 102 (1980) 92–98, https://doi.org/10.1021/ja00521a016, American Chemical Society.

[66] O.T. Sililo, J.H. Tellam, Fingering in unsaturated zone flow: a qualitative review with laboratory experiments on heterogeneous systems, Groundwater 38 (2000) 864–871, https://doi.org/10.1111/j.1745-6584.2000.tb00685.x, https://onlinelibrary.wiley.com/doi/abs/10.1111/j.1745-6584.2000.tb00685.x, https://onlinelibrary.wiley.com/doi/pdf/10.1111/j.1745-6584.2000.tb00685.x.

[67] C. Soulaine, J. Maes, S. Roman, Computational microfluidics for geosciences, Front. Water 3 (2021), https://doi.org/10.3389/frwa.2021.643714, https://www.frontiersin.org/articles/10.3389/frwa.2021.643714.

[68] V.M. Starov, Surfactant solutions and porous substrates: spreading and imbibition, Adv. Colloid Interface Sci. 111 (2004) 3–27, https://doi.org/10.1016/j.cis.2004.07.007, https://www.sciencedirect.com/science/article/pii/S0001868604000491.

[69] V.M. Starov, S.R. Kostvintsev, V.D. Sobolev, M.G. Velarde, S.A. Zhdanov, Spreading of liquid drops over dry porous layers: complete wetting case, J. Colloid Interface Sci. 252 (2002) 397–408, https://doi.org/10.1006/jcis.2002.8450, https://www.sciencedirect.com/science/article/pii/S002197970298450X.

[70] U. Thiele, Recent advances in and future challenges for mesoscopic hydrodynamic modelling of complex wetting, Colloids Surf. A, Physicochem. Eng. Asp. 553 (2018) 487–495, https://doi.org/10.1016/j.colsurfa.2018.05.049, https://www.sciencedirect.com/science/article/pii/S0927775718304175.

[71] U. Thiele, S. Hartmann, Gradient dynamics model for drops spreading on polymer brushes, Eur. Phys. J. Spec. Top. 229 (2020) 1819–1832, https://doi.org/10.1140/epjst/e2020-900231-2.

[72] U. Thiele, M.G. Velarde, K. Neuffer, Y. Pomeau, Film rupture in the diffuse interface model coupled to hydrodynamics, Phys. Rev. E 64 (2001) 031602, https://doi.org/10.1103/PhysRevE.64.031602, https://link.aps.org/doi/10.1103/PhysRevE.64.031602, American Physical Society.

[73] M.G. Wallis, D.R. Scotter, D.J. Horne, An evaluation of the intrinsic sorptivity water repellency index on a range of New Zealand soils, Soil Res. 29 (1991) 353–362, https://doi.org/10.1071/sr9910353, https://www.publish.csiro.au/sr/sr9910353, CSIRO Publishing.

[74] X. Xu, U. Thiele, T. Qian, A variational approach to thin film hydrodynamics of binary mixtures, J. Phys. Condens. Matter 27 (2015) 085005, https://doi.org/10.1088/0953-8984/27/8/085005, https://dx.doi.org/10.1088/0953-8984/27/8/085005, IOP Publishing.

[75] I.M. Zickenrott, S.K. Woche, J. Bachmann, M.A. Ahmed, D. Vetterlein, An efficient method for the collection of root mucilage from different plant species—a case study on the effect of mucilage on soil water repellency, J. Plant Nutr. Soil Sci. 179 (2016) 294–302, https://doi.org/10.1002/jpln.201500511, https://onlinelibrary.wiley.com/doi/abs/10.1002/jpln.201500511, https://onlinelibrary.wiley.com/doi/pdf/10.1002/jpln.201500511.